ELSEVIER

Bioelectrochemistry 52 (2000) 161–167

Bioelectrochemistry

www.elsevier.com/locate/bioelechem

Membrane-permeabilizing activities of cyclic lipodepsipeptides, syringopeptin 22A and syringomycin E from *Pseudomonas syringae* pv. *syringae* in human red blood cells and in bilayer lipid membranes

Gabriella Agner [a], Yuri A. Kaulin [b], Philip A. Gurnev [b], Zsofia Szabo [a], Ludmila V. Schagina [b], Jon Y. Takemoto [c], Katalin Blasko [a,*]

[a] *Institute of Biophysics and Radiation Biology, Semmelweis University of Medicine, POB 263, Budapest VIII, Puskin u. 9, 1444 Budapest, Hungary*
[b] *Institute of Cytology, Russian Academy of Sciences, St. Petersburg, Russia*
[c] *Department of Biology, Utah State University, Logan, UT, USA*

Received 23 December 1999; received in revised form 29 May 2000; accepted 31 May 2000

Abstract

The pore-forming activities of cyclic lipodepsipeptides (CLPs), syringopeptin 22A (SP22A) and syringomycin E (SRE) were compared on the human red blood cell (RBC) membrane and on bilayer lipid membranes (BLMs). SP22A above a concentration of 4×10^5 molecules/cell significantly increased the RBC membrane permeability for ^{86}Rb. With electric current measurements on BLM, it was proved that like SRE, the SP22A formed two types of ion channels in the membrane, small and large, the latter having six times larger conductance and longer dwell time. Both CLPs formed clusters consisting of six small channels, and the channel-forming activity of SP22A is about one order of magnitude higher than that of SRE.

A Hill coefficient of 2–3 estimated from the concentration dependence of these CLPs-induced lysis gave a proof of the pore oligomerization on RBCs. Transport kinetic data also confirmed that SP22A pores were oligomers of at least three monomers. While SRE pores were inactivated in time, no pore inactivation was observed with SP22A. The ^{86}Rb efflux through SP22A-treated RBCs approached the tracer equilibrium distribution with a constant rate; a constant integral current was measured on the BLM for as long as 2.5 h as well. The partition coefficient ($K_p = 2 \times 10^4$ l/mol) between the RBC membrane and the extracellular space was estimated for SRE to be at least six times higher than that for SP22A. This finding suggested that the higher ion permeability of the SP22A-treated cells compared to that of SRE was the result of the higher pore-forming activity of SP22A.

Keywords: Syringomycin E; Syringopeptin 22A; Pore formation; Pore inactivation; Red blood cell membrane; Bilayer lipid membrane

1. Introduction

The phytopathogenic bacterium *Pseudomonas syringae* pv. *syringae* produces two different classes of cyclic lipodepsipeptides (CLPs): (i) the lipodepsinonapeptides syringomycins (SRs) and related nonapeptides (syringotoxins and syringostatins) and (ii) syringopeptins (SPs). Both kinds of CLPs are composed of a polar peptide head and a hydrophobic 3-hydroxy-fatty-acid tail [1–4]. The most effective representative of the first group, syringomycin E (SRE) has a peptide head consisting of a lactone ring built up by nine, mainly hydrophilic amino-acid residues [2,3,5]. Four of the nine amino acids are charged, resulting in the two positive net charges of the molecule. Syringopeptins contain a larger peptide moiety with 22 (syringopeptin 22A (SP22A) and syringopeptin 22B (SP22B)) or 25 (syringopeptin 25A (SP25A) and syringopeptin 25B (SP25B)) amino-acid residues, from which only eight form a polar lactone ring with two positive net charges; the remaining are hydrophobic amino-acid residues and the fatty-acid parts [4,6].

Both SRE and SPs have important roles in the virulence of the bacterium *P. syringae* pv. *syringae*. SRE was shown to induce necrosis in different plant tissues [7,8]. SRE and SPs promoted stomatal closure in leaves of *Xanthium strumarium* [9], lysed tobacco protoplasts [10],

Abbreviations: BLM, bilayer lipid membrane; BS solution, buffered salt solution; CLP, cyclic lipodepsipeptide; DOPE, 1,2-dioleoyl-*sn*-glycero-3-phosphoethanolamine; DOPS, 1,2-dioleoyl-*sn*-glycero-3-phosphoserine; H, haematocrit; MOPS, 3-(*N*-morpholino)-propanesulfonic acid; RBC, red blood cell; SP22A, syringopeptin 22A; SPs, syringopeptins; SRE, syringomycin E; SRs, syringomycins

* Corresponding author. Tel.: +36-1-266-6656; fax: +36-1-266-6656.
E-mail address: blasko@puskin.sote.hu (K. Blasko).

0302-4598/00/$ - see front matter
PII: S0302-4598(00)00098-2

caused necrosis of tobacco leaves [11] and electrolyte leakage of carrot tissues [12], and inhibited the plasma-membrane ATPase activity of maize root [13]. In all of these effects, SPs were found to be more active than SRE. Both CLPs have antifungal effect against pathogenic fungi with different spectra of antimicrobial activity [12,14,15].

The antifungal and plant pathogenic effects of these lipopeptids are reported to be related to pore formation in the host membrane leading to cytolysis [6,10,16]. SRE and SPs were observed to cause haemolysis of red blood cells (RBCs) of different origin probably by the colloid osmotic mechanism [10,17]. Sorensen et al. [14] reported that SRE induced lysis of sheep erythrocytes. Hutchison and Gross [10] compared the hemolytic effect of SRE and SP22A/SP22B on horse RBCs and found that the lytic activity of SP22A ($\approx$ that of SP22B) is about 85% of that of SRE. However, Dalla Serra et al. [16] reported the hemolytic activity of SRE on human and rabbit RBCs to be about one order of magnitude higher than that of SP22A ($\approx$ SP25A). In contrast, Lavermicocca et al. [12] found SP22A and SP25A to be more active than SRE in the hemolytic effect on sheep erythrocytes. In all of these experiments, the lytic effect was measured to show the pore-forming activities of these compounds.

In planar bilayer lipid membranes (BLM), SRE-induced pores with weak anion selectivity were reported [17–21]. It was shown that SRE forms two types of channels (large and small ones) and the large SRE channels are clusters of the small ones exhibiting synchronous opening and closing [18,19]. The SRE pore radius was found to be concentration-dependent [16] ranging from 0.7 up to 1.7 nm. Hutchison and Gross [10] showed SP22B-formed pores in planar lipid bilayers. Dalla Serra et al. [16] suggested SP22A pores to be oligomers of 3–6 monomers, and estimated the pore radius of 0.88 nm to be independent of the concentration of the peptide.

In our previous work [22,23], we showed on human RBCs that SRE induced haemolysis of a fraction of cells in a concentration-dependent manner and enhanced the permeability of lysis-survived cells for ^{86}Rb and monomeric haemoglobin. With ion-transport kinetic measurements, it was proved that SRE formed pores in RBC membranes; the pores had discrete life times and were eventually inactivated.

In this paper, transport kinetic studies were performed at body temperature and at nearly physiological haematocrit values to compare the pore-forming activities of SRE and SP22A in human RBCs. The channel-forming activity of SP22A was also measured on BLMs and compared with that of SRE.

2. Materials and methods

Human blood from healthy volunteers was stabilized with citrate buffer and stored at 4°C for up to 3 days. Synthetic 1,2-dioleoyl-*sn*-glycero-3-phosphoserine (DOPS) and 1,2-dioleoyl-*sn*-glycero-3-phosphoethanolamine (DOPE) were purchased from Avanti Polar Lipids (Pelham, AL). SP22A and SRE were purified to homogeneity as described earlier [24] and stored frozen. All chemicals used were of analytical grade.

2.1. ^{86}Rb efflux

Blood was loaded with ^{86}Rb for 1.5 h at 37°C. After centrifugation, the RBCs were washed three times with buffered salt (BS) solution (in mmol/l): 3.2 KCl, 138 NaCl, 1 $CaCl_2$, 1 $MgCl_2$, 27 sucrose, 5 3-(*N*-morpholino)-propanesulfonic acid (MOPS), (pH 6.8) and then resuspended into the same solution. The RBC suspension was kept at 37°C.

SP22A (4 mg/ml in 10^{-3} mol/l HCl) or SRE (2 mg/ml in 10^{-3} mol/l HCl) stock solutions were diluted with 6 ml of BS solution. An RBC suspension (14 ml) and the diluted SP22A/SRE solution were mixed with rigorous stirring. The initial haematocrit values (H) of the RBC suspension were between 0.4 and 0.5, the SP22 concentrations were in the range of 4×10^5–1×10^8 molecules/cell (17–4300 μg/ml RBCs), the SRE concentrations were 4×10^6–2.4×10^7 molecules/cell (100–600 μg/ml RBCs). The suspension was incubated at 37°C in a shaking water bath. Samples of the suspension were taken at designated time intervals. The samples were centrifuged and the radioactivity of aliquots of the supernatant fluids was measured with a γ scintillation counter (Gamma, Hungary).

^{86}Rb transport was characterized by the amount of tracer found in the supernatant fluids after a time period t and expressed as the percentage of the total activity of the suspension (N_t). The tracer efflux was presented in an N_t-versus-t curve as well as in a semilogarithmic plot: $-\ln(1 - N_t/N_\infty)$ over time, where N_∞ was the percentage of radioactivity in the external medium at the tracer equilibrium state. With SRE, the number of modified cells (m) was calculated as described previously [22] and N_∞ (mod), the saturation level of the transport was taken as the level of tracer equilibrium between the SRE-modified cells and the extracellular space. The slopes of the curves were proportional to the rate constant of efflux of the tracer cation. From the rate constant (k), the permeability coefficient of the membrane (p) was calculated using the formula:

$$p = \frac{kV_iV_o}{S(V_i + V_o)} \quad (1)$$

where S is the total area of modified cell membranes, calculated as a product of the number of modified cells (m) in 1-ml cell suspension and the surface area of one cell (1.37×10^{-6} cm^2) [25], V_o is the extracellular volume

of a 1-ml cell suspension ($V_o = (1 - H)$), and V_i is the intracellular volume of modified cells ($V_i = m0.68V$, where V is the mean cell volume) [26].

RBC concentration and haematocrit value (H) were determined based on electric-impedance measurement using an automated hematology analyzer (COBAS MICROS OT 18, Roche, France). The CLP-induced haemolysis was calculated as the difference between the RBC concentrations of the untreated (A_o) and CLP-treated (A) RBC suspensions and expressed as a percentage of A_o.

2.2. Determination of the partition coefficient

The partition coefficient (K_p), the ratio of the bound CLP in the outer monolayer of the RBC membrane and the free one in the extracellular solution [27], was calculated from the CLPs-induced lysis obtained at different haematocrit values. For the calculation, the following assumptions were made: (i) K_p was independent of the H value, (ii) the same amount of bound CLP in the outer membrane monolayer caused the same extent of lysis. K_p was calculated using the formula:

$$K_p = \frac{(1 - H_2) M_1 - (1 - H_1) M_2}{L(A_1 M_2 - A_2 M_1)}, \quad (2)$$

where M_1 and M_2 are the amounts of CLPs added to the RBC suspension at H_1 and H_2 haematocrit values, respectively to obtain the same percentage of lysis, A is the number of RBCs in a 1-l RBC suspension, L is the amount of lipids in the outer monolayer of the membrane of one RBC (3.75×10^{-16} mol/cell [28]).

2.3. Measurements of single-channel current and conductance on BLM

Virtually solvent-free membranes were prepared as described by Montal and Muller [29]. Bilayer membranes were formed from an equimolar mixture of DOPS and DOPE in hexane. The BLM was bathed in 100 mmol/l NaCl, 5 mmol/l MOPS (pH 6). Two symmetrical halves of a Teflon chamber with solution volumes of 1 cm^3 were divided by a 15-μm-thick Teflon partition containing a round aperture of about 100-μm diameter. Hexadecane in *n*-hexane (1:10, v/v) was used for the aperture pretreatment. A pair of Ag–AgCl electrodes was used to maintain membrane potential and to detect current fluctuations. "Virtual ground" was maintained at the *trans* side of the bilayer. Positive currents are therefore those of cations flowing from *cis* to *trans* [18,20]. Bilayer formation was indicated by the subsequent increase in membrane capacitance to its final value of 80–100 pF. Measuring the bilayer's conductance checked their stability. For unmodified bilayers, a conductance value of about 1 pS was found which remained unchanged under conditions chosen during several hours. SP22A or SRE was added to the aqueous phase at one (*cis*) side of the bilayer from stock solutions (1 mg/ml in 10^{-3} mol/l HCl)), and the current records began 10 min later to allow the system to equilibrate. Details on membrane preparation, single-channel and membrane-current measurements may be found elsewhere [30].

3. Results and discussion

SP22A added to the RBCs at 37°C, above the concentration of 4×10^5 molecules/cell (17 μg/ml RBCs), increased the membrane permeability for ions as monitored by direct measurement of ^{86}Rb (a tracer analog of the K^+ ion) efflux (Fig. 1). Fig. 1(a) shows the time courses

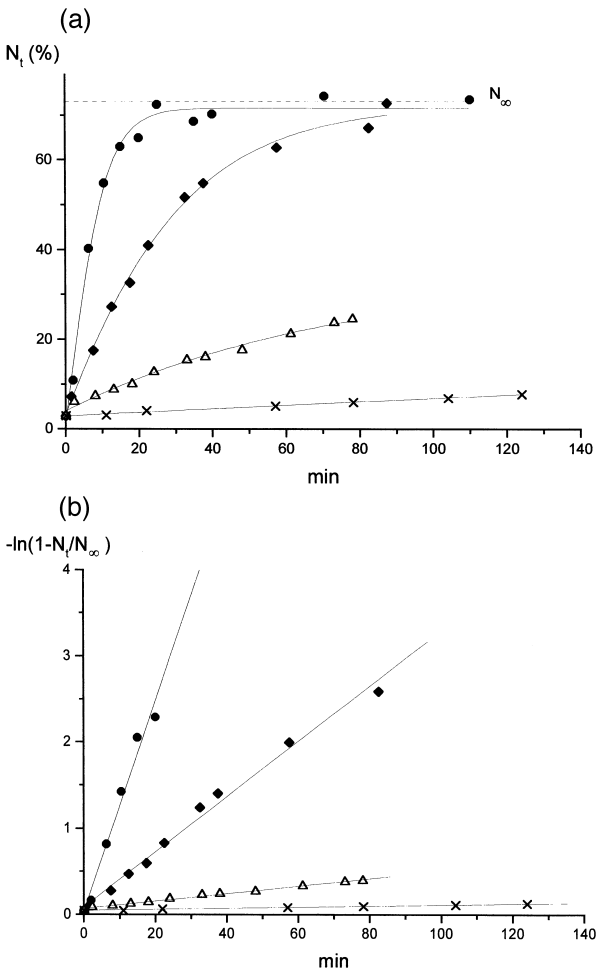

Fig. 1. (a) Concentration dependence of SP22A-induced ^{86}Rb efflux through RBC membranes. RBCs were suspended in BS solution (in mmol/l: 3.2 KCl, 138 NaCl, 1 $CaCl_2$, 1 $MgCl_2$, 27 sucrose, 5 MOPS (pH 6.8), temperature 37°C). The ordinate gives the amount of radioactive ions effluxed, expressed as the percentage of the total activity of the RBC suspension (N_t). N_∞ is the percentage amount of ^{86}Rb in the extracellular solution at tracer equilibrium. SP22A concentrations in molecules/cell (μg/ml RBCs): × 0, △ 4×10^5 (17), ♦ 7.2×10^5 (28), ● 1.1×10^6 (43). SP22A was added at 0 min. (b) Semilogarithmic representation of the kinetic data given in (a).

of ^{86}Rb efflux at different SP22A concentrations. ^{86}Rb efflux increased with time and approached the equilibrium tracer distribution between the intra- and extracellular spaces. This suggests that all cells have pores in their membranes. Below the concentration of 1×10^6 molecules/cell there was no measurable lysis of cells during the time that the transport reached the equilibrium.

A semilogarithmic plot of the ^{86}Rb efflux curves (Fig. 1(b)) showed that one exponent fit the data of the kinetic curves indicating the ^{86}Rb efflux to be a diffusion process through the SP22A-formed pores. In the concentration of 7×10^5 molecules/cell it took 80 min until the transport reached the equilibrium distribution. However, no change in the transport rate was observed during that time (Fig. 1(b)) suggesting that in contrast with SRE pores [23], the SP22A pores did not inactivate during this time period.

From the slope of the transport curves, the permeability coefficients (p_{Rb}) were calculated. A typical concentration–effect curve is shown in Fig. 2. The permeability increased with the third power of the SP22A concentration. Though the absolute response of certain concentrations of SP22A varied, the slopes of the curves (logarithm of p_{Rb} versus the logarithm of the concentration of SP22A) in all cases were in the range of 2–4 (3 ± 1). This fact suggests that at least three monomers of SP22A are needed to form a pore.

In contrast with SP22A, SRE caused a rapid (within 2 min) lysis of a minor portion of the RBCs, the extent of this lysis remained unchanged for as long as 100 min (see Fig. 1 in Ref. [22]). The SRE-induced ^{86}Rb efflux increased with time and then ceased at a level far from the equilibrium tracer distribution between the intra- and extracellular spaces (Fig. 3). This kind of transport kinetics (see also Fig. 6 in Ref. [22] and Fig. 1 in Ref. [23]) was explained by the presence of two subpopulations of lysis-survived cells: the so-called unmodified cells, which have only small pores in their membranes and SRE-modified cells having pores in cluster form [18,23]. Thus, the saturation level of transport was considered as the level of tracer equilibrium between the SRE-modified cells and the extracellular space. From the semilogarithmic representation of the data of ^{86}Rb efflux through SRE-modified cells (Fig. 4(b)), a rate constant of 8.3×10^{-2} min^{-1} was obtained, and a permeability coefficient $p = 5.7 \times 10^{-8}$ cm/s was calculated. Such a permeability coefficient value was obtained with SP22A at four times less concentration.

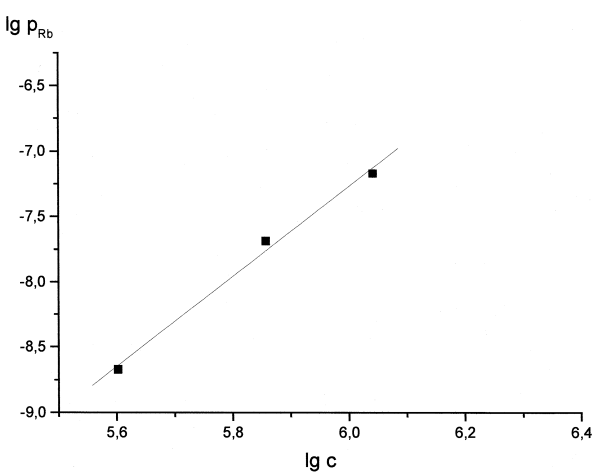

Fig. 2. Concentration dependence of the permeability coefficients (p_{Rb}) of SP22A-treated RBC membranes. The permeability coefficients were calculated from the slopes of lines presented in Fig. 1(b). For experimental conditions, see Fig. 1.

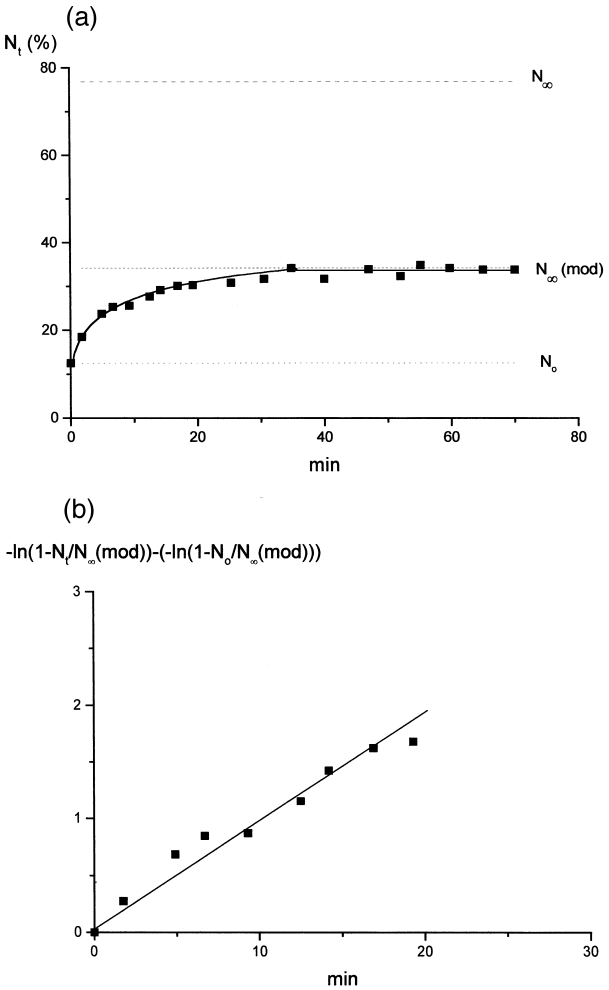

Fig. 3. (a) Time course of ^{86}Rb efflux through RBC membranes treated with SRE in a concentration of 4×10^6 molecules/cell (100 μg/ml RBCs) at 37°C. RBCs were suspended in BS solution (for composition, see Fig. 1). The ordinate gives the amount of radioactive ions effluxed, expressed as the percentage of the total activity of the RBC suspension (N_t). N_∞ is the percentage amount of ^{86}Rb in the extracellular solution at tracer equilibrium between the extracellular space and the intracellular space of all lysis-survived cells. N_∞ (mod) is the percentage amount of ^{86}Rb in the extracellular solution at tracer equilibrium between the intracellular solution of modified cells and the extracellular solution. N_o is the percentage value of the ^{86}Rb due to lysis and contamination. SRE was added at 0 min. (b) Semilogarithmic representation of the kinetic data given in (a).

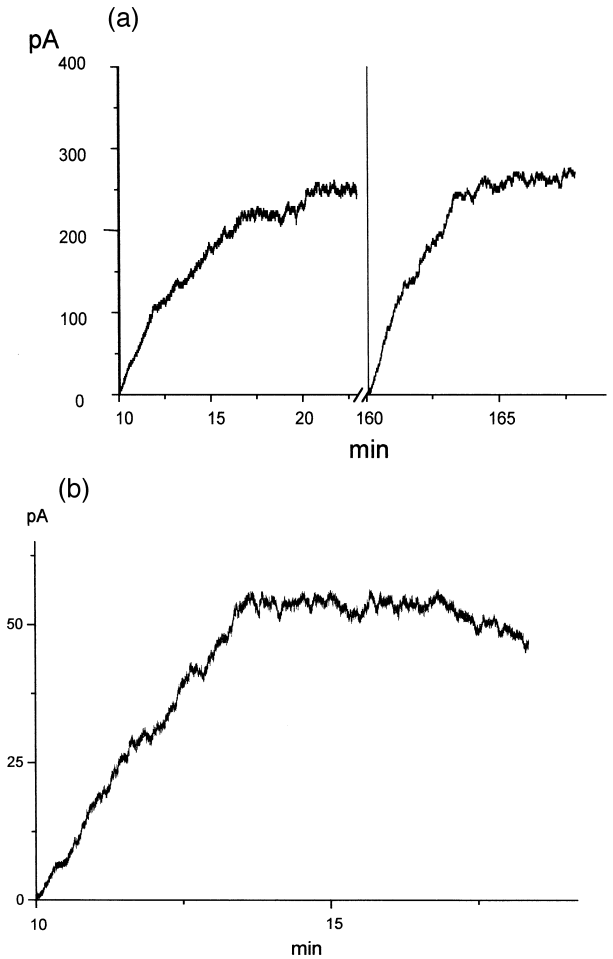

Fig. 4. Time courses of the membrane current through bilayers doped with SP22A (a) and SRE (b) recorded at an applied voltage of 50 mV. Membrane bathing solutions were: 100 mmol/l NaCl (pH 6) at 20°C. The membranes were formed from a lipid mixture of DOPS/DOPE (1:1, M:M). SP22A and SRE were added to the bathing solution (*cis* side only) in a concentration of 0.2 and 2 μg/ml, respectively at $t = 0$ min.

The kinetics of ion (^{86}Rb) transport curves reflected the differences in the pore-forming activities of these CLPs at body temperature and at a nearly physiological haematocrit value. In order to have experimental support that SP22A pores also form clusters in RBC membranes, the concentration dependence of SP22A lysis was measured and found to be sigmoidal and quite steep. From the Hill representation, a Hill coefficient of 2.6 ± 0.4 was obtained indicating oligomerization of not less than three monomers. This finding is in agreement with that of Dalla Serra et al. [16] and with our results obtained from the tracer-permeability data.

With SRE, however, a linear relationship of the ^{86}Rb transport rate with SRE concentration was obtained in our previous work at room temperature [22]. The time-dependent inactivation of SRE pores [23] might be reason of this relationship, which prevented determination of the oligomerization of SRE pores. In order to clarify that SRE oligomers form pores in RBCs at body temperature, lysis

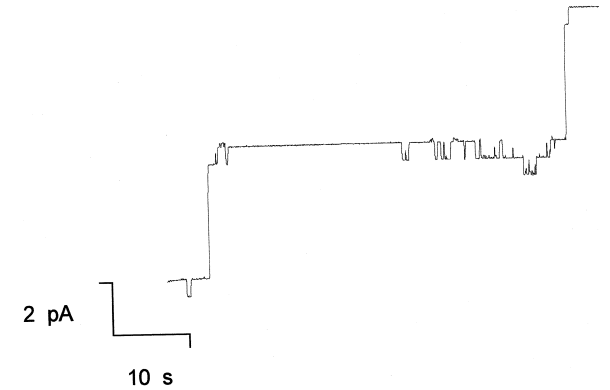

Fig. 5. The records of current fluctuations at −150 mV transmembrane potential of SP22A modified bilayers at 22°C. Salt concentration was 100 mmol/l NaCl (pH 6). The membrane was formed from a lipid mixture of DOPS/DOPE (1:1, M/M). SP22A was added to the bathing solution (*cis* side only) in a concentration of 0.2 μg/ml.

was measured at 37°C in the concentration range of 4×10^6–2.4×10^7 SRE molecules/cell. The curve was fitted to the Hill equation, and the resulting Hill coefficient was 2.1. This value indicates oligomerization especially if we consider that the Hill coefficient underestimates the number of monomers in the oligomer [16,31]. Thus, it is suggested that the same kind of SRE pore formed in RBC membranes at body temperature as is found in the bimolecular lipid membrane at room temperature [16–18,20].

To study the SP22A pore formation and the pore properties, electrical measurements were performed on BLMs made from an equimolar mixture of phosphatidylserine and phosphatidylethanolamine, a negatively charged and a neutral phospholipid of RBC membrane, and modified by SP22A. The same membrane composition was used in our previous experiments with SRE [23].

Fig. 4(a) shows the time course of the integral current through the bilayer membranes in the presence of SP22A. At a positive potential, the membrane current increased

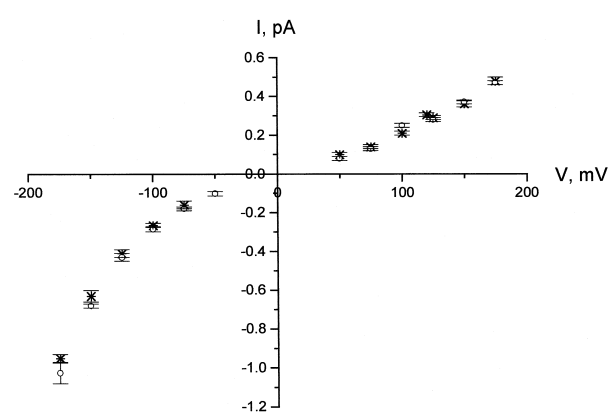

Fig. 6. Voltage–current curves for SRE and SP22A small channels. ○ — SRE, ∗ — SP22A. For experimental conditions, see Fig. 5. The concentrations of SRE and SP22A in the bathing solutions (*cis* side only) were 2 and 0.2 μg/ml, respectively.

and a stable current was registered for about 15 min. Then negative potential was applied, inducing the closing of the channels (not shown) [20]. After 130 min, the same positive transmembrane potential was applied, and the current increased up to the same level indicating that unlike the SRE pores [23] there was no time-dependent inactivation of SP22A pores during 2.5 h. In order to compare the channel-forming activities of SP22A and SRE, the integral bilayer current was measured in the presence of SRE (Fig. 4(b)). Comparison of the curves in Fig. 4(a) and (b) reveals that the current through SRE-modified BLM at saturation level at the same transmembrane potential was smaller than that for SP22A-treated bilayers even though the concentration of SRE was 10 times higher than the concentration of SP22A (2 versus 0.2 μg/ml).

The single-channel recording (Fig. 5) shows that SP22A formed similar pores as SRE [18,19]. Two types of channels were registered (small and large) that are different in conductance by a factor of six-fold. The dwell time of the large channels was greater than that of the small ones. Fig. 6 shows the voltage–current curves for SRE and SP22A small channels. Identical current values were obtained for pores formed from both CLPs in the voltage range from -175 to $+175$ mV. Thus, the properties of SRE and SP22A channels are essentially the same. It indicated that similar to SRE [18,19], the large SP22A channels were clusters of six small ones with simultaneous opening and closing.

On the other hand, the p_{Rb} for SRE-treated RBCs (at a concentration of 4×10^6 molecules/cell) was equal to 5.7×10^{-8} cm/s, which was similar to that estimated for RBCs treated with SP22A at about four times less concentration. The higher permeability for ^{86}Rb of the SP22A-modified membrane may be explained by a larger partition coefficient of SP22A between the RBC membrane and the extracellular solution related to that of SRE, or a higher pore-forming activity of SP22A in the membrane. Both factors result in an increased number of pores. In addition to this, the lower ^{86}Rb-transport rate with SRE may be due to a decreasing number of pores in time as a result of pore inactivation. The SRE partition coefficient between the RBC membrane and the extracellular space was determined and a K_p of 2×10^4 l/mol was obtained. For SP22A, a six-times-less K_p (3×10^3 l/mol) was estimated. This means that at a given concentration of these modifiers, more SRE molecules are in the RBC membrane than in SP22A. Thus, the higher permeability of the SP22A-treated cells compared to that of SRE is proved to be the result of the higher pore- and cluster-forming activity of SP22A.

Acknowledgements

This research was supported by grants from the Hungarian Health Ministry (ETT, No. 486/96), the Russian Ministry of Sciences (No. 8f), the Russian Fund for Basic Research (No. 00-04-49386) and the Utah Agricultural Experiment Station (Project UTA 00607).

References

[1] D.C. Gross, J.E. De Vay, F. Stadman, Chemical properties of syringomycin and syringotoxin: toxigenic peptides produced by *Pseudomonas syringae*, J. Appl. Bacteriol. 43 (1977) 453–463.
[2] A. Segre, R.C. Bachmann, A. Ballio, F. Bossa, I. Grgurina, N.S. Iacobellis, G. Marino, P. Pucci, M. Simmaco, J.Y. Takemoto, The structure of syringomycins A1, E and G, FEBS Lett. 255 (1989) 27–31.
[3] N. Fukuchi, A. Isogai, J. Nakayama, S. Takayama, S. Yamashita, K. Suyama, J.Y. Takemoto, A. Suzuki, Structure and stereochemistry of three phytotoxins, syringomycin, syringotoxin and syringostatin, produced by *Pseudomonas syringae* pv. *syringae*, J. Chem. Soc., Perkin Trans. 1 (1992) 1149–1157.
[4] A. Ballio, D. Barra, F. Bossa, A. Collina, I. Grgurina, G. Marino, G. Moneti, M. Paci, P. Pucci, A. Segre, M. Simmaco, Syringopeptins, new phytotoxic lipodepsipeptides of *Pseudomonas syringae* pv. *syringae*, FEBS Lett. 291 (1991) 109–112.
[5] E. Vaillo, A. Ballio, P.-L. Luisi, R.M. Thomas, The spectroscopic properties of the lipodepsipeptide, syringomycin E, Biopolymers 32 (1992) 1317–1326.
[6] C.L. Bender, F. Alarcon-Chaidez, D.C. Gross, *Pseudomonas syringae* phytotoxins: mode of action, regulation, and biosynthesis by peptide and polyketide synthetases, Microbiol. Mol. Biol. Rev. 63 (1999) 266–292.
[7] S.L. Sinden, J.E. DeVay, P.A. Backman, Properties of syringomycin, a wide spectrum antibiotic and phytotoxin produced by *Pseudomonas syringae*, and its role in the bacterial canker disease of peach trees, Physiol. Plant Pathol. 1 (1971) 199–213.
[8] D.C. Gross, J.E. DeVay, Role of syringomycin in holcus spot of maize and systemic necrosis of cowpea caused by *Pseudomonas syringae*, Physiol. Plant Pathol. 11 (1977) 1–11.
[9] D. Di Giorgio, L. Camoni, K.A. Mott, J.Y. Takemoto, A. Ballio, Syringopeptins, *Pseudomonas syringae* pv. *syringae* phytotoxins, resemble syringomycin in closing stomata, Plant Pathol. 45 (1996) 564–571.
[10] M.L. Hutchison, D.C. Gross, Lipopeptide phytotoxins produced by *Pseudomonas syringae* pv. *syringae*: comparison of the biosurfactant and ion channel-forming activities of syringopeptin and syringomycin, Mol. Plant–Microbe Interact. 10 (1997) 347–354.
[11] N.S. Iacobellis, P. Lavermicocca, I. Grgurina, M. Simmaco, A. Ballio, Phytotoxic properties of *Pseudomonas syringae* pv. *syringae* toxins, Physiol. Mol. Plant Pathol. 40 (1992) 107–116.
[12] P. Lavermicocca, N.S. Iacobellis, M. Simmaco, A. Graniti, Biological properties and spectrum of activity of *Pseudomonas syringae* pv. *syringae* toxins, Physiol. Mol. Plant Pathol. 50 (1997) 129–140.
[13] L. Camoni, D. DiGiorgio, M. Marra, P. Aducci, A. Ballio, *Pseudomonas syringae* pv. *syringae* phytotoxins reversibly inhibit the plasma membrane H+-ATPase and disrupt unilamellar liposomes, Biochem. Biophys. Res. Commun. 214 (1995) 118–124.
[14] K.N. Sorensen, K.-H. Kim, J.Y. Takemoto, In vitro antifungal and fungicidal activities and erythrocyte toxicities of cyclic lipodepsinonapeptides produced by *Pseudomonas syringae* pv. *syringae*, Antimicrob. Agents Chemother. 40 (1996) 2710–2713.
[15] A.J. De Lucca, T.J. Jacks, J.Y. Takemoto, B. Vinyard, J. Peter, E. Navarro, T.J. Walsh, Fungal lethality, binding, and cytotoxicity of syringomycin-E, Antimicrob. Agents Chemother. 43 (1999) 371–373.
[16] M. Dalla Serra, G. Fagiuoli, P. Nordera, I. Bernhart, C. Della Volpe, D. Di Giorgio, A. Ballio, G. Menestrina, The interaction of lipodepsipeptide toxins from *Pseudomonas syringae* pv. *syringae* with

biological and model membranes: a comparison of syringotoxin, syringomycin, and two syringopeptins, Mol. Plant–Microbe Interact. 12 (1999) 391–400.
[17] M.L. Hutchison, M.A. Tester, D.C. Gross, Role of biosurfactant and ion channel-forming activities of syringomycin in transmembrane ion flux: a model for the mechanism of action in the plant–pathogen interaction, Mol. Plant–Microbe Interact. 8 (1995) 610–620.
[18] Y.A. Kaulin, L.V. Schagina, S.M. Bezrukov, V.V. Malev, A.M. Feigin, J.Y. Takemoto, J.H. Teeter, J.G. Brand, Cluster organization of ion channels formed by the antibiotic syringomycin E in bilayer lipid membranes, Biophys. J. 74 (1998) 2918–2925.
[19] L.V. Schagina, Y.A. Kaulin, A.M. Feigin, J.Y. Takemoto, J.G. Brand, V.V. Malev, Properties of ionic channels formed by the antibiotic syringomycin E in lipid bilayers: dependence on the electrolyte concentration in the bathing solution, Membr. Cell Biol. 12 (1998) 537–555.
[20] A.M. Feigin, J.Y. Takemoto, R. Wangspa, J.H. Teeter, J.G. Brand, Properties of voltage-gated ion channels formed by syringomycin E in planar lipid bilayers, J. Membr. Biol. 149 (1996) 41–47.
[21] A.M. Feigin, L.V. Schagina, J.Y. Takemoto, J.H. Teeter, J.G. Brand, The effect of sterols on the sensitivity of membranes to the channel-forming antifungal antibiotic, syringomycin E, Biochim. Biophys. Acta 1324 (1997) 102–110.
[22] K. Blasko, L.V. Schagina, G. Agner, Y.A. Kaulin, J.Y. Takemoto, Membrane sterol composition modulates the pore forming activity of syringomycin E in human red blood cells, Biochim. Biophys. Acta 1373 (1998) 163–169.
[23] G. Agner, Y.A. Kaulin, L.V. Schagina, J.Y. Takemoto, K. Blasko, Effect of temperature on the formation and inactivation of syringomycin E pores in human red blood cells and bimolecular lipid membranes, Biochim. Biophys. Acta 1466 (2000) 79–86.
[24] A.P. Bidwai, L. Zhang, R.C. Bachmann, J.Y. Takemoto, Mechanism of action of *Pseudomonas syringae* pv. *syringae* phytotoxin, syringomycin. Stimulation of red beet plasma membrane ATPase activity, Plant Physiol. 83 (1987) 39–43.
[25] K.G. Engstrom, B. Moller, H.J. Meiselman, Optical evaluation of red blood cell geometry using micropipette aspiration, Blood Cells 18 (2) (1992) 241–265.
[26] O. Sten-Knudsen, Passive transport processes, in: G. Giebish, D.C. Tosteson, H.H. Ussing (Eds.), Membrane Transport in Biology, Springer, Berlin, 1978, pp. 5–114.
[27] D. Rapaport, R. Peled, S. Nir, Y. Shai, Reversible surface aggregation in pore formation by pardaxin, Biophys. J. 70 (1996) 2502–2512.
[28] S.R. Hollan, J.H. Breuer, J.G. Szelényi, On the red cell membrane, Haematologia 6 (1972) 221–236.
[29] M. Montall, P. Muller, Formation of bimolecular membranes from lipid monolayers and a study of their electrical properties, Proc. Natl. Acad. Sci. U. S. A. 69 (1972) 3561–3566.
[30] S.M. Bezrukov, I. Vodyanoy, Probing alamethicin channels with water-soluble polymers. Effect on conductance of channel states, Biophys. J. 64 (1993) 16–25.
[31] J.N. Weiss, The Hill equation revisited: uses and misuses, FASEB J. 11 (1997) 835–841.